Modelling back face deformation of woven layered composite targets under oblique impact

Marina Seidl, Norbert Faderl, Marvin Becker

ISL - French-German Research Institute of Saint-Louis
5 Rue du Général Cassagnou, 68300 Saint-Louis

Abstract

Body armour is the only protection a dismounted soldier has against projectiles or fragments in case of combat. Perforation is prevented in body armour as the kinetic energy of the projectile is transformed to deformation work in the armour material. This dynamic material response upon impact is especially crucial for helmets, as it acts directly on the human head. One potential threat nowadays a foot soldier faces during missions is the *7.62x39 mm* projectile fired from a rifle. Helmets are not designed to withstand a direct impact of such a projectile, which is launched at an initial velocity of v_i*=720+/10 m/s*. Under an obliquity angle of θ*>65 degrees* (NATO) projectile ricocheting is observed. The aim of the ongoing project is to promote the projectile ricochet off helmets to increase the likelihood of projectile deflection and the survivability of the wearer. The focus of this paper is the target back-face deformation (BFD) upon oblique high velocity impact. Experiments were conducted on projectile impact on plane aramid plates. These plates have the same material properties, such as layer number, as used for manufactured helmets – other ballistic helmet materials are covered in future research. Upon impact, the dynamic BFD of the aramid targets was measured, using digital image correlation (DIC). Additionally, the experiments were repeated to capture the projectile trajectory through the target thickness, using X-ray cinematography. The BFD and trajectory results are used for the qualitative comparison of a numerical model, defined within the LS-DYNA® explicit Lagrangian solver. Model components, the projectile and target plate are defined using fully integrated hexahedral elements. The projectile deformation is represented by **`*MAT_JOHNSON_COOK`** and its failure criterion; and the target plate is represented by **`*MAT_COMPOSITE_DAMAGE`**. The projectile and the composite target are in a symmetric contact defined by **`*CONTACT_ERODING_SURFACE_TO_SURFACE`**. The aim of this paper is an investigation on the most suitable modelling approach for a numerical validation of the BFD response obtained from the DIC measurements. This work is a first step to implementing experimentally and numerically achieved BFD data in a LS-DYNA® Finite element (FE) head model, using a head injury criteria (HIC).

Keywords: Finite Element (FE) Method, High velocity impact, layered composites, back face deformation, X-ray cinematography, Head injury criteria (HIC)

Abbreviations

ATP	**A**ramid **T**arget **P**late
BFD	**B**ack **F**ace **D**eformation
CAD	**C**omputer **A**ided **D**esign
deg	**Deg**ree
DIC	**D**igital **I**mage **C**orrelation
DOF	**D**egree **O**f **F**reedom
EOS	**E**quation **O**f **S**tate
HIC	**H**ead **I**njury **C**riteria
FEM	**F**inite **E**lement **M**ethod
FPS	**F**rames **P**er **S**econd
FXRIP	**F**lash **X**-**R**ay **I**mage **P**rocessing
ISL	French-German Research **I**nstitute of **S**aint-**L**ouis
NATO	**N**orth **A**tlantic **T**reaty **O**rganisation
VPAM	**V**ereinigung der **P**rüfstellen für **a**ngriffshemmende **M**aterialien und Konstruktionen

1 Introduction

Almost sixty years ago, DuPont introduced a new aramid fibre, marketed under the trade name Kevlar®. Due to its high strength and low weight, Kevlar® represented a breakthrough of synthetic composite materials [1] and is presently, an even more valued material for lightweight application and ballistic protection.
The aramid yarns – an agglomeration of fibres – are woven into layers, using diverse yarn weaving patterns to enhance certain material characteristics [2]. The manufacturing of body armour, particularly ballistic helmets, starts with the chosen number of woven fibre layers, which are cut into various shapes. These woven aramid shapes are positioned into a press for helmet molding. During the molding process, woven aramid layers are bonded to epoxy matrices, where the fibre-matrix adhesion is of utmost importance [3]. Due to this material complexity, each finished aramid composite helmet is unique. From the fibre direction to its adhesion with the epoxy material, everything affects the material response under impact conditions. Aramid composites are not the only material used for ballistic helmets, e.g. UHMWPE (ultra-high-molecular-weight polyethylene). However, this paper focuses on the projectile impact on woven fibre aramid. The complexity of composite materials leads to challenges in the repeatability of experiments. Not only is it a difficult task to properly determine the accurate impact position on the helmet for ballistic tests, the differences in the aramid composites, due to the production process, remain uncertain as well. Therefore, a certain error band is expected in the experimental results. This uncertainty in the experimental repeatability makes the numerical approach essential. It is common to use aramid target plates (ATP), manufactured using the same material as the helmet shell. Consistent fibre direction and plane plate impact simplify experiments, especially on oblique impact. However, the drawbacks of the target simplifications are of lower back face deformation (BFD) values, as the ATP material response is geometry dependent.
This investigation covers a *7.62 x 39 mm* projectile impact with a *70 deg (NATO)* obliquity. The BFD using DIC is measured. Additionally, first tests have been successful in capturing the projectile trajectory, utilising the new X-ray cinematography system. This data is used for numerical model validations. Composite material modelling has been widely studied in the past, describing different approaches, such as varying element types [4] [5]. Parametric studies have led to the current model description and are still ongoing. The objective of this paper is to present a discussion of the challenges in numerical model validation, using DIC data obtained upon oblique impact. This work is part of a continuing project in which this experimentally and numerically obtained BFD of a helmet is implemented in a HIC model, so that the prediction of potential injuries to the wearer is possible in the future [6] [7] [8].

2 Experiments

2.1 Set-up

Experiments were conducted in the ballistic laboratory of the ISL. Three tests at initial velocities of *500, 600* and *700 m/s* at are chosen and the projectile was shot at an angle of *70 deg (NATO)*. NATO degree angles are measured from the target perpendicular to the projectile rotational axis (Fig. 1).

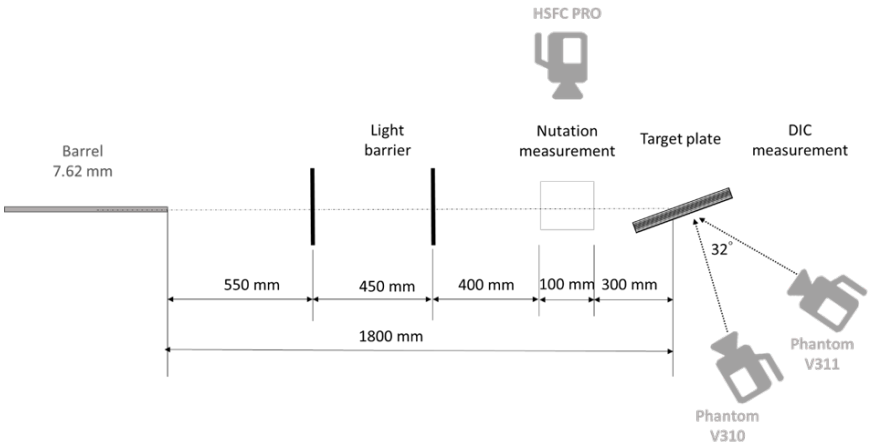

Fig. 1: Experimental set-up for 7.62x39 mm oblique impact on aramid target plates (ATP)

The ATPs are supplied by a helmet manufacturer and have the same aramid material composition as combat helmets. The barrel muzzle is positioned *1800 mm* from the ATP impact position, p_{im}, and is closer than the regulation allowed distance, such as the VPAM (Fig. 1). Due to the limited flight distance, the projectile trajectory is captured by a HSFC Pro high speed camera. It monitors the projectile nutation (Fig. 5). The initial projectile velocity v_i is measured with light barriers. Upon impact, the BFD is captured using DIC (Fig. 2). The plastic deformation on the plate is shown in Fig. 3.

2.2 Results

2.2.1 Dynamic deformation – DIC

DIC is an optical method for measuring 2D or 3D coordinates for the evaluation of deformation, such as displacement and strain. For the 3D measurement, two high speed cameras are placed at an angle to the specimen. The DIC picture frame consists of *512 x 384* pixels, with *15000 fps* and *4 µs* exposure time. The whole principal is based on stochastic patterns, which are applied on the measuring objects. A software computes 3D coordinates on the pattern, obtained from the two cameras, for individual images. Deformed patterns represent a deformed object and the BFD is obtained through the DIC measurements. For high velocity impacts, the often-suggested approach of using spray paint for the stochastic pattern does not work, as the colour spalls off upon impact and the measurement is corrupted. A black marker ink was used instead. Additionally, the contrast between measured surface and pattern is important, as a higher contrast provides more stable DIC measurements. Both cameras are positioned at a distance far enough to allow for the coverage of the area of interest, yet no too far to ensure enough resolution. For the best results, the camera should be positioned perpendicular to the measured surface, however, that is not always possible. Especially in the case of expected projectile ricochet, the system needs to be away from a probable residual projectile trajectory.

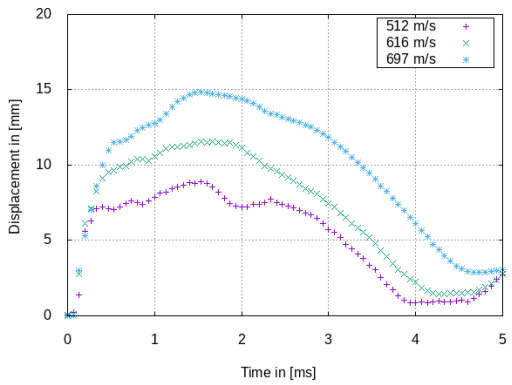

a) BFD at p_{im}

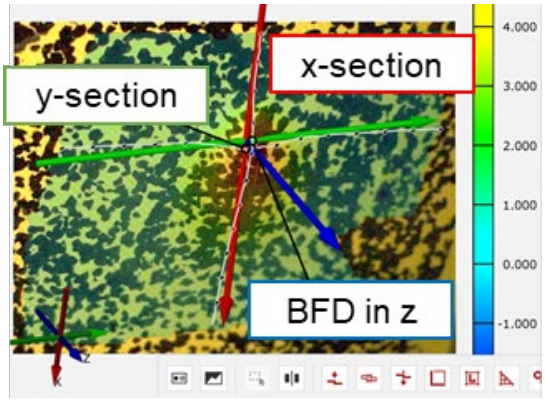

b) Screenshot of GOM for 512 m/s

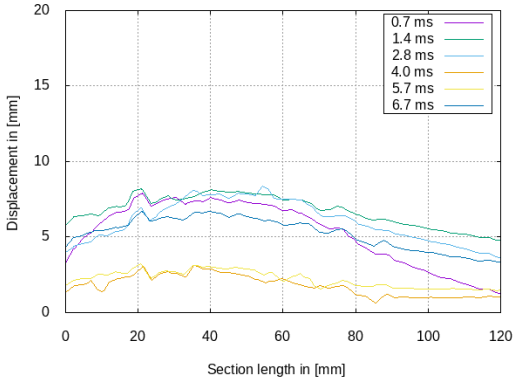

c) BFD in x-section for 512 m/s

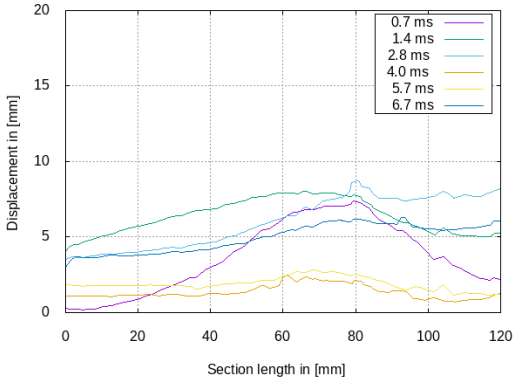

d) BFD in y-section for 512 m/s

Fig. 2: BFD measured with DIC, a) displacement in impact point for 3 tested velocities, b) screenshot of measurement (numerical model see Fig. 7), c) BFD in x-section (red)

Fig. 2 summarises the results obtained from the DIC and visualized in the GOM-correlate software. The first graph in Fig. 2a shows the displacement of a chosen point for all three measurements. The point is defined in an area of first measured stochastic pattern displacement. Unlike a perpendicular impact at *0 deg (NATO)*, the p_{im} and the maximum BFD do not correspond upon oblique impact (Fig. 4a). At higher velocities, the BFD signature changes and a BFD comparison for different velocities is ongoing. Shown are the exemplary displacements in the vertical (Fig. 2c) and horizontal (Fig. 2d) directions. For the first step towards future evaluations of numerical models, a maximum averaged BFD value, as shown in Fig. 2a, is obtained and found in Tab. 1

Tab. 1: Plastic and dynamic deformation of ATP

Test no	Initial velocity	Plastic BFD			Front face	Dynamic BFD
	v_i in m/s	x in mm	y in mm	z in mm	f in mm	in mm
1	512	40 +/- 10	50 +/- 10	10 +/- 5	25 +/- 5	8+/- 2
2	616	60 +/- 10	85 +/- 10	15 +/- 5	35 +/- 5	11 +/- 2
3	697	75 +/- 10	85 +/- 10	20 +/- 5	70 +/- 5	15 +/- 2

2.2.2 Plastic deformation

The remaining plastic deformation on the ATP is summarised in Tab. 1. The maximal horizontal (x-direction) and vertical (y-direction) directions describe the area and the height (z-direction) of the visible remaining bulge. A more sophisticated approach is the measurement of the deformation signature, which is planned for future work. The length *f*, in which the projectile travelled during ricochet inside the material, is shown on the front face. Unlike what was observed of the BFD measurement in helmets and curved aramid shapes, where the dynamic is up to double the remaining (or plastic) BFD, here the values are similar inside the error band.

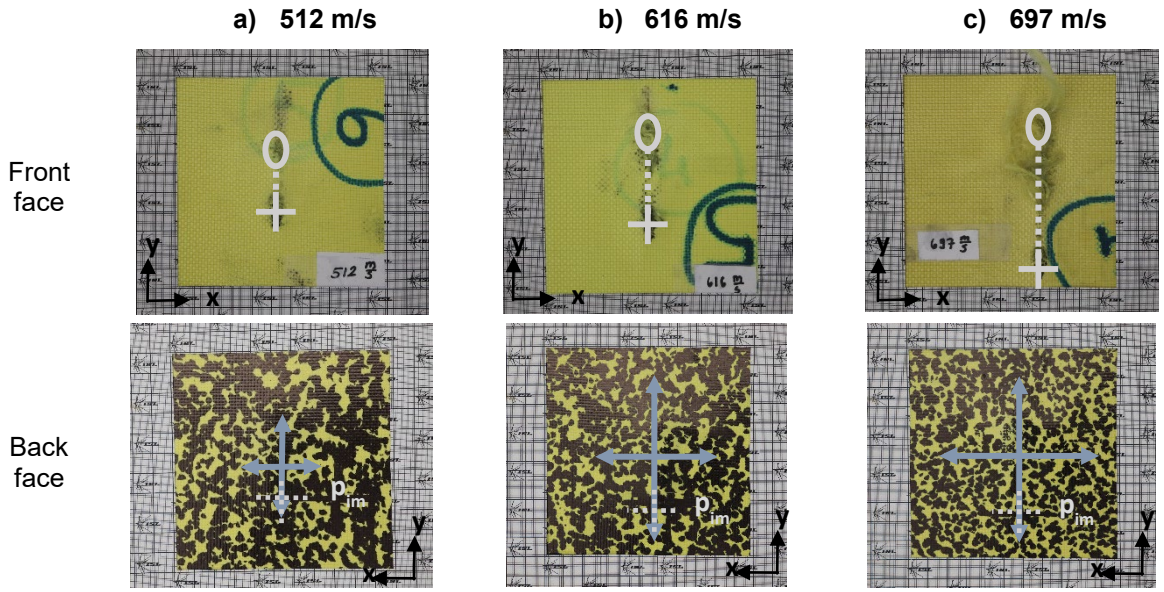

Fig. 3: Plastic deformation of aramid target with a) 512 m/s; b) 616 m/s and c) 697 m/s

The impact of the front face is shown in the upper images of Fig. 3. The cross marks the projectile impact point p_{im}, where the projectile penetrates the ATP. A dotted line marks the distance were the projectile travelled inside the ATP layers. The exit is marked with a circle, as its position is not as clearly determined as the p_{im}.
In the second row (Fig. 3), the corresponding remaining BFD is shown. The horizontal blue lines indicate the x-direction and the vertical lines the y-direction, respectively. A dotted cross shows the impact position, p_{im}.

2.2.3 X-ray cinematography

X-ray cinematography uses one multi-anode tube – instead of several separate X-ray tubes – which are circularly arranged. It captures up to eight separate images [9]. This configuration causes a parallax for the projections from the different anodes, thus a FXRIP software has been developed [10]. Three points are needed for the affine transformation and are employed during experiments (Fig. 4a). Fig. 4b shows a transformed state with the parallax eliminated, while the maximum BFD occurs after the projectile has exited the ATP (Fig. 4c). Additional image post-processing, such as rotational velocities, is possible (Fig. 4d) [11]

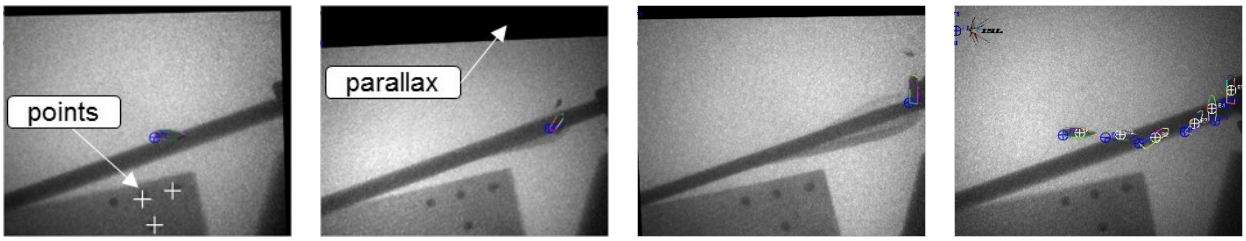

a) 0 µs b) 50 µs c) 100 µs d) all at Δt=50 µs

Fig. 4: X-ray cinematography results on trajectory of 7.62x39 mm with 512 m/s

2.2.4 Projectile nutation

The results from the HSFC Pro high-speed camera measurement show that the *7.62x39 mm* projectile stabilises at the short flight distance, and a possible nutation (pitch and yaw angle) can be neglected. Below are the results for test 1, with v_i*=512 m/s* (Fig. 5). The projectile travels from left to right of the image.

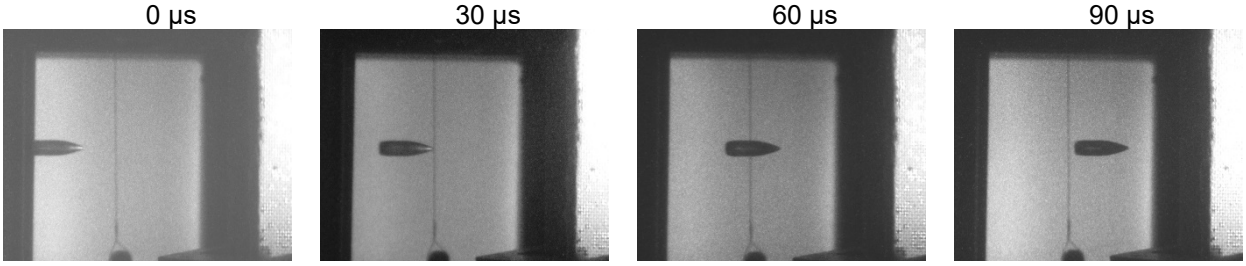

Fig. 5: High speed video results of 7.62x39 mm flight trajectory launched with 512 m/s

3 Numerical model

LS-DYNA® solver R 8.1, with symmetric multiprocessing (SMP) and double precision, was used for all the calculations. The model consists of five parts; three parts describe the projectile – lead filler, steel core and brass jacket. The composite target is defined by two parts. Uneven numbered layers belong to part one and the even numbered to the other part, respectively.

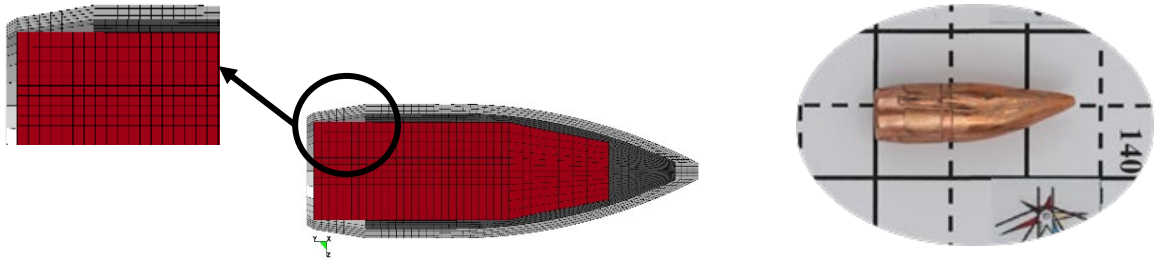

a) Meshed 7.62x39 mm projectile b) Deformation after impact

Fig. 6: 7.62x39 mm projectile

3.1 Projectile

The projectile is modelled with three components, the core, the lead, and the jacket. The full projectile modelling approach is chosen for this early stage. Simplifications in the projectile modelling approach required additional parameter studies, especially when the full projectile is later implemented in the simulation. The projectile has a blunt core which enhances the ricochet capability. During tests, it was repeatedly observed, on different configurations that the jacket stays fully intact [12]. A slight deformation of the lead-filled nose tip was the occurring damage (Fig. 6).

3.1.1 Mesh and boundary conditions

Fig. 6 shows the 7.62x39 mm projectile section view. It is meshed from CAD model with the LS-DYNA® block mesh function. The lead is not fully meshed until the projectile end due to decreasing mesh size. All parts are connected with a **`*CONTACT_SURFACE_TO_SURFACE_EROSION`**. A **`*PART_SET`** is defined and applied with **`*INITIAL_VELOCITY`**. Further boundary conditions are not applied.

3.1.2 Material

The projectile components were modelled with **`*MAT_JOHNOSON_COOK`** material and failure parameters [13]. The Von Mises stress flow stress σ_y is given in the equation below.

$$\sigma_y = \left(A + B\bar{\varepsilon}^{p^n}\right)\left(1 + c \cdot ln(\dot{\varepsilon}^*)\right)\left(1 - T^{*m}\right) \quad (1)$$

$\bar{\varepsilon}_p$ is the effective plastic strain and $\dot{\varepsilon}^* = \bar{\varepsilon}_p / \varepsilon_0$ is the dimensionless plastic strain rate. Constant *A* is the yield stress. The strain hardening effects of the material are represented by constant *B* and exponent *n*. The strain rate effect is expressed through constant *C* and exponent *m* represents temperature softening of the material through homologous temperature $T^*=(T-T_0)/(T_m-T_0)$. *T* is the absolute temperature, T_0 is the room temperature and T_m is the melting temperature of the target material [14] [15]. Failure is defined by the ε^f is the equivalent plastic fracture strain.

$$\varepsilon^f = \left(D_1 + D_2 e^{D_3 \sigma^*}\right)\left(1 + D_4 \cdot ln(\dot{\varepsilon}^*)\right)\left(1 + D_5 T^*\right) \quad (2)$$

D_1, D_2, D_3, D_4, and D_5 are fracture model constants. The defined parameters are summarised in Tab. 2

A Mie-Grueneisen EOS defines solid pressure state. The general definition is

$$P - P_H = \frac{\gamma}{v}(E - E_H) \quad (3)$$

With reference state H (one point on the Hugoniot) and the Grueneisen parameter γ.

Tab. 2: Johnson-Cook constitutive model constants [16]

	Elastic constants and density			**Yield stress and strain hardening**			**Strain rate hardening**	
	G [GPa]	**v []**	**ρ [g/cm³]**	**A [MPa]**	**B [MPa]**	**n**	**$\dot{\varepsilon}$ [s⁻¹]**	**C**
Core	79.6	0.3	7.85	234.4	413.8	0.25	1	0.0033
Lead	5.6	0.43	11.34	10.3	41.3	0.21	1	0.0033
Jacket	40	0.43	8.96	448.2	303.4	0.15	1	0.0033

	Adiabatic heating and temperature softening			**Fracture strain constants**				
	c_p [J/kgK]	**T_m [K]**	**T_0 [K]**	**m**	**D_1**	**D_2**	**D_3**	**D_4**	**D_5**
Core	4.5	1800	293	1.03	5.625	0.3	-7.2	-0.0123	0
Lead	1.29	328	293	1.03	0.25	0	0	0	0
Jacket	3.86	1356	293	1.03	2.25	0.0005	-3.6	-0.123	0

Previous numerical tests of the projectile material parameters showed that the literature material parameters had a softer response than the used projectile [17]. Different reasons can cause that discrepancy; the first probably is that although a through constitutive material parametric study was

published [16], some missing parameters for the EOS and temperature softening were taken from other sources [18]. Moreover, projectiles are not measurement instruments and changes in material configurations differ. The material parameter fitting is ongoing in this research.

3.2 Woven layered composite target

There are different ways to model woven layered composites. They are split into micro-, meso- and macro-scale models. Micro-scale models represent each fibre and simulate the interaction between those. Meso-scale models represent one fibre crossing per element. Usually micro-scale boundary conditions are transferred to the meso-scale. Macro-scale covers multiple fibre crossings. This approach was the most reasonable for the model set-up due to calculation costs

3.2.1 Mesh and boundary conditions

The composite plate consists of a quadratic mesh in the centre at *80 x 100 mm* and is extended by a *50 mm* bias mesh. The smallest element size in the quadratic centre is *0.8 mm*, which is larger than previous studies [12] [17]. Each layer has a *0.375 mm* thickness and is represented by two element rows. The layer thickness was calculated by dividing the sample thickness with the layer number. Instead of defining a small gap between the layers and connecting them with a ***TIEBREAK_SURFACE_TO_SURFACE** contact [17], the layers were attached by merging the contact nodes. In later investigations about the BFD and delamination, the merged nodes approach was not sufficient. Furthermore, the material parameters described in the literature are defined with an additional matrix material [5]. Therefore, the merged node definition is mostly set to simplify parametric studies (Fig. 8).
Boundary nodes on the plate edge have no translational DOF set in the ***CONSTRAINED_BOUNDARY_SPC**. According to literature, delamination is better represented in layered woven composites without constrained nodes [19]. Previous work has discussed the boundary conditions on the ATP [17], that the numerical model is large enough to influence, due to boundary conditions because of which the constrained nodes are negligible. Tests showed that the presence of defined boundary conditions led the calculation time to be up to 30% faster, than without (SMP with 2 threads) [17].

3.2.2 Discussion on the element choices

First, the question is about whether to use the ***ELEMENT_SHELL**, ***ELEMENT_TSHELL,** or the ***ELEMTN_SOLID** elements. The ***ELEMENT_TSHELL** are modelled with two element rows per layer to avoid extensive softness [20]. As the ricochet occurrence strongly depends on the target material stresses in the normal direction [21], the ***ELEMENT_SOLID** were the focus of this paper to describe the ricochet phenomenon, which occurs in the beginning, for up to *100 µs* (Fig. 4). The BFD is the ATP material response to the projectile ricochet, and experiments show that its maximum value arises at *1-2 ms (1000-2000 µs)* for plates, and similarly for helmets as well [12]. However, DIC over predicts the BFD as first, only the helmet shell can be captured, and second, the head will stop further deformation. Hence, the numerical model so far focuses on the first occurrence of projectile ricochet and uses ***ELEMENT_SOLID.**

3.2.3 Material

The approach was a macro-scale model using the composite damage material description ***MAT_COMPOSITE_DAMAGE**. The literature provided the material parameters [5], and a successful application to the high velocity projectile impact has been discussed [4].

Tab. 3: Composite material parameters.

Elastic properties						
Density [g/cm^3]	**Young's Moduli [GPa]**		**Shear Moduli [GPa]**		**Poisson's ratio []**	
ρ	E_A, E_B	E_C	G_{BA}	G_{CA}, G_{BC}	ν_{BA}	ν_{CA}, ν_{BA}
1.23	18.5	6.0	0.77	*5.43*	0.25	0.33
Strength properties						
Tensile [MPa]		**Compressive [MPa]**		**Shear [MPa]**		
X_T, Y_T	S_N	Y_C		S_{YZ}, S_{ZX}	S_C	
555.0	34.5	1200.0		*543.0*	9.0	

According to the literature, the composite parameters were adjusted [22]. The elastic shear modulus is doubled to *10.86 GPa* and the shear strength is halved to *2.72 GPa* [22].

4 Discussion and comparison

4.1 Parametric study

Fig. 8a shows the initial state of the front and side few, at *t=0 µs*. The result upon *7.62x39 mm* projectile impact at *512 m/s* and at *70 deg (NATO)* obliquity is shown in Fig. 8b. In this state, the comparison to plastic deformation (Fig. 3) is not done using the current model set-up. The runtime would need to be extended to *1000-2000 µs,* and longer. This model focuses on the projectile behaviour. Further investigations on the material behaviour and results on the BFD will be included in future work.
When changing the material parameters, as it has been described in literature [22], the results go up to *100 µs* (Fig. 8c). Some minor changes in the material behaviour become evident. So far, the projectile trajectory was not influenced by material changes in the investigated timeframe. Differences in material response, by restarting the same model using eight instead four threads, is demonstrated by comparing Figs. 8b and 8d. Further steps in changing the precision, and material model to obtain more stable results, independent of the solver setting, are planned.

4.2 X-ray cinematography

When comparing the X-ray cinematography (Fig. 4) to the numerical model (Fig. 8 section views), it was seen that the projectile rotation inside the material could be captured. A qualitative comparison was possible at this stage, which helped in the understanding of the ricochet phenomenon of the complex ATP material. The projectile ends the contact at about *100 µs* for v_i*=512 m/s,* where the BFD occurs at about *1000 µs* in the material.

4.3 Comparability to DIC

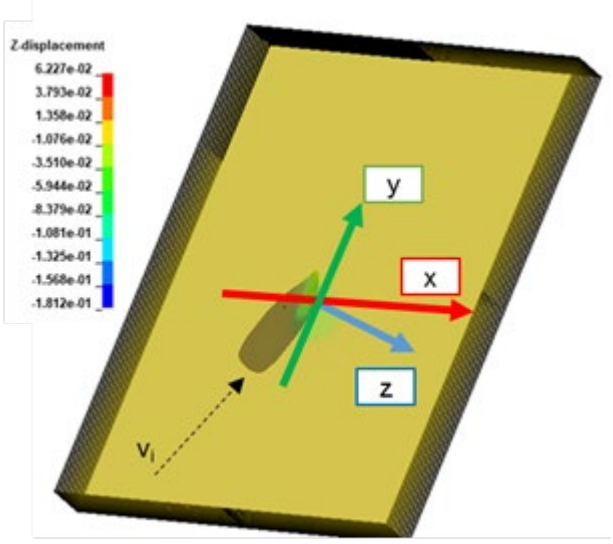

Fig. 7: Numerical model comparison of initial position definition

Fig. 7 shows a simulation at *t=10 µs*, with a coordinate system positioned as in the DIC measurement (Fig. 2). The projectile is shown at impact. For future successful numerical and experimental data comparison, a few points need to be investigated:
First, the experimentally and numerically defined coordinate system to compare the BFD results may not correlate. DIC cameras show the image from an angle (Fig. 1) and the coordinate system may be distorted.
Second, the point of impact p_{im} can be very precisely determined in the numerical model, yet not experimentally. The p_{im} is hidden at the strike face, and the origin of the coordinate system is placed where the first BFD was measured.
Third, the initial time is set experimentally at first measurement, at the back face. Numerically, the projectile comes in contact with the plate at the initial state.

5 Future Steps

The numerical model is evaluated and developed on plane ATP and after sufficient validation is used for the shaped complex helmet structures. The projectile and the target plates are under future development. The projectile material parameters are under investigation. The material response is softer than expected from experimental results. Further contact settings between the components are planned. Parametric studies for contact between the aramid layers as well as an implementation of a matrix material are planned. Further material models, such as **`*MAT_SOLID_COMPOSITE_FAILURE,`** will be used and compared. Obtained and validated material data is implemented in a helmet shell mesh and added to a HIC model. Material studies, such as padding performance under projectile impact, can be performed, and a better insight on protection capabilities can be obtained.

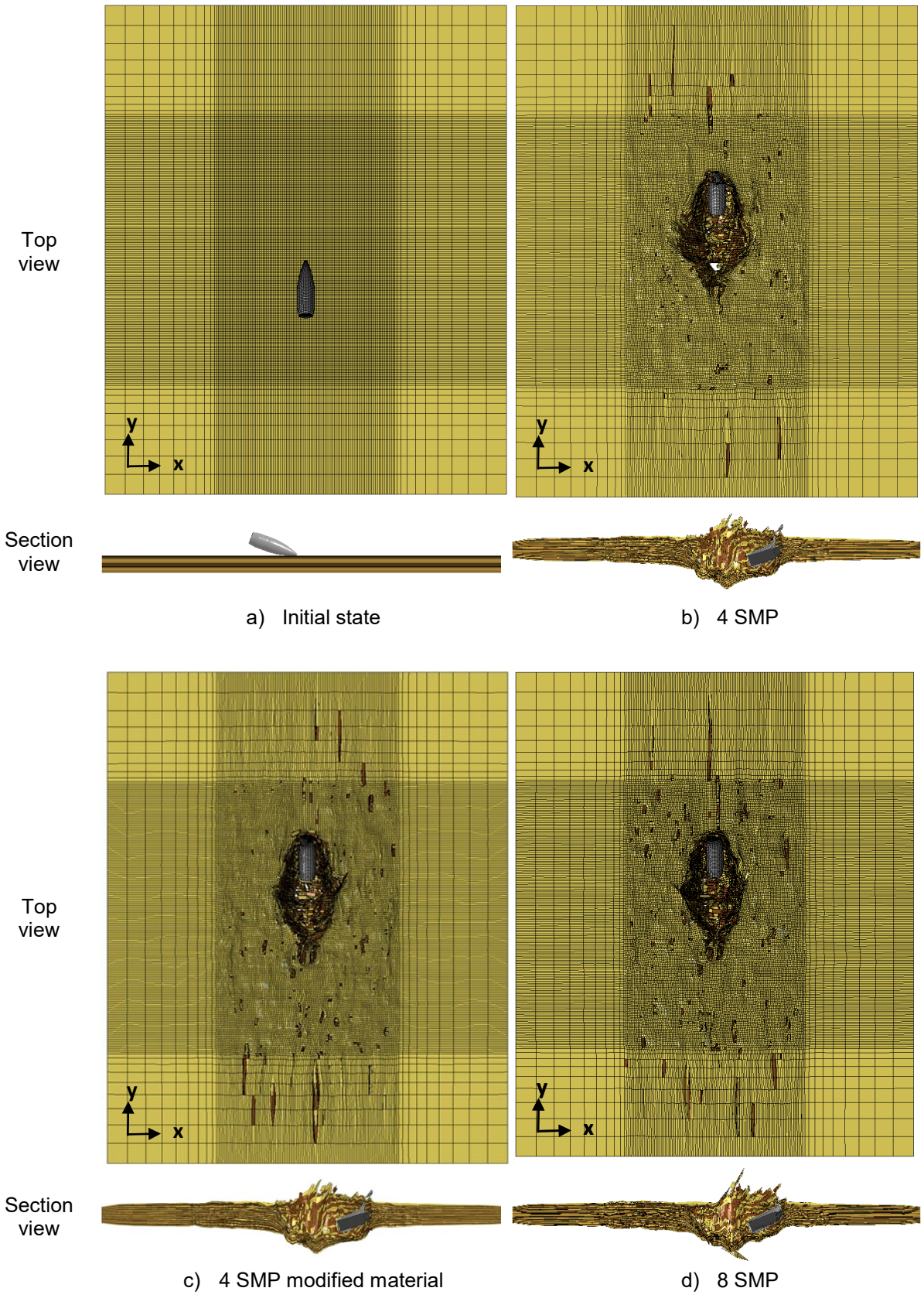

Fig. 8: Impact at 70 deg (NATO) a) Initial state at t=0 µs b); result with 4 SMP threads at t=100 µs c) model of b) with changed material properties; d) model of b) with 8 SMP threads

6 Summary

This paper demonstrates the current status of an ongoing project. The experimental part discusses the measurement capabilities upon an oblique, *7.62x39 mm* impact on ATPs. DIC is used for the target response, and X-cinematography is utilised for an investigation of the projectile trajectory. The complexity of the problem shows the current challenges of experimental data evaluations, such as a BFD comparison obtained at different impact velocities. Numerical model evaluation, and the development accompanying the experimental tests, support a better physical understanding. The quantitative model validations show that projectile behaviour during the penetration process of the ATP can be captured successfully.

7 Acknowledgements

This study contributes to the project HNBi (www.hnbi.eu) and is co-financed by the European Regional Development Fund (ERDF) and the Region Grand-Est.

8 Literature

[1] RC, Review of Department of Defense, “Test Protocols for Combat Helmets”, Washington D.C, U.S.: National Research Council (NRC), National Academies Press, 2014

[2] Chu C.-K. and Chen Y.-L., „Ballistic-proof Effects of Various Woven,“ Fibres & Textiles in Eastern Europe, 18(6)2010: 63-7.

[3] Kalantar J. and Drzal L. T., „The bonding mechanism of aramid fibres to epoxy matrices - Part 1“, J. Mater. Sci, 25(1)1990:4186-93.

[4] Aare M., „Evaluation of head response to ballistic helmet impacts using FEM“, J. Imp. Eng., 34(1)2007:596-608.

[5] van Hoof J., „Modelling of impact induced delamination in composite materials“, Carleton University, Ottawa, Canada, 1999.

[6] Baumgartner D and R. Willinger, „Finite element modelling of human head injuries caused by ballistic projectiles“, Revue Européenne des Éléments Finis, 14(4-5)2005:559-76.

[7] Deck C. and Willinger R., „Improved head injury criteria based on head FE model“, Int. J. of Crashworthiness , 13(6)2018:667-78.

[8] Raul J.-S., Deck C., Willinger R. and Ludes B., „Finite-element models of the human head and their applications in forensic practice“, Int. J. of Legal Medicine, 122(5)2008:359-66.

[9] Strassburger E., Bauer S., Weber S. and Gedon H., „Flash X-ray cinematography analysis of dwell and penetration of small caliber projectiles with three types of SiC ceramics“, Defence Technology, 12(3)2016:277-83.

[10] Becker M., „FXRIP - Flash X-Ray Image Processing and Analyzing Software for Ballistic Impact Applications“, ISL, Saint-Louis, France, 2018.

[11] Becker M., „Extraction the Rotational Velocity of Fragments from X-Ray Images Using Object Tracking Algorithms“, ISL, Saint-Louis, France, 2018.

[12] Seidl M., „Ricochet off helmets“, in PASS, Washington D.C., USA, 2018.

[13] Johnson G. and Cook W. H., „A constitutive model and data for metals subjected to large strains, high strain rates and high temperatures“, in Proceedings of the 7th International Symposium on Ballistics, The Hague, Netherlands, 1983.

[14] Brar, N. S. et al., „Constitutive Model Constants for Al7075T651 and Al7075T6“, AIP Conference Proceedings, 2009:1195-945.

[15] Seidl M., Wolf T. and Nuesing R., „Numerical ricochet investigation of spin-stabilized projectile on plane armour steel targets“, in LS-DYNA® User Conference, Salzburg, Austria, Mai 2017.

[16] Carbajal L., Jovicic J. and Kuhlmann H., „Assault Rifle Bullet-Experimental Characterization and Computer (FE) Modelling“, in Society for Experimental Mechanics, Uncasville, Connecticut, US, 2011.

[17] Seidl M., Ramezani A. and Linz L., „Investigations on ricochet off complex targets – woven layered composite“, in Nordic LS-DYNA® Conference, Gothenburg, Sweden, 2018.

[18] Adams B., “Simulation of ballistic impacts”, Eindhoven, NL: Eindhoven University of Technology, 2003.

[19] Stuehmeyer A., „The thick shell element for metal forming and other applications“, in 5th European LS-DYNA User Conference, Birmingham, UK, 2005.

[20] Rosenberg Z. and Dekel E., „Terminal Ballistics“, Haifa, Israel: Springer-Verlag, 2012.

[21] van Hoof J., Deutekom M. J., Worswick M. J. and M. Bolduc, „Experimental and numerical analysis of the ballistic impact response of composite helmet materials“, in 18th ISB, San Antonio, USA, 1999.